Investigation of quantum dot passively mode-locked lasers with excited-state transition

Hsu-Chieh Cheng* and Chien-Ping Lee

Department of Electronics Engineering, National Chiao Tung University, 1001 University Road, Hsinchu 30010, Taiwan

* *u890851@alumni.nthu.edu.tw*

Abstract: Monolithic passively mode-locked quantum dot lasers with excited-state transition were investigated in a broad operating range without ground-state lasing. Optical and electrical characteristics of these mode locked lasers were studied in detail at different levels of injection current and absorber bias. Very different behaviors in the evolution of the hysteresis, the optical spectra and the evolution of repetition frequency were observed between our lasers and conventional quantum dot lasers with ground-state transition. Possible mechanisms behind these observed phenomena were proposed and discussed. A minimum pulse width of 3.3 ps and an externally compressed pulse width of 0.78 ps were obtained.

OCIS codes: (140.5960) Semiconductor lasers; (140.4050) Mode-locked lasers.

References and links

1. A. Markus, J. X. Chen, O. Gauthier-Lafaye, J. G. Provost, C. Paranthoën, and A. Fiore, "Impact of intraband relaxation on the performance of a quantum-dot laser," IEEE J. Sel. Top. Quantum Electron. **9**(5), 1308–1314 (2003).
2. A. Markus, M. Rossetti, V. Calligari, D. Chek-Al-Kar, J. X. Chen, A. Fiore, and R. Scollo, "Two-state switching and dynamics in quantum dot two-section lasers," J. Appl. Phys. **100**(11), 113104 (2006).
3. H. Y. Wang, H. C. Cheng, S. D. Lin, and C. P. Lee, "Wavelength switching transition in quantum dot lasers," Appl. Phys. Lett. **90**(8), 081112 (2007).
4. S. Schneider, P. Borri, W. Langbein, U. Woggon, R. L. Sellin, D. Ouyang, and D. Bimberg, "Excited-state gain dynamics in InGaAs quantum-dot amplifiers," IEEE Photon. Technol. Lett. **17**(10), 2014–2016 (2005).
5. D. B. Malins, A. Gomez-Iglesias, S. J. White, W. Sibbett, A. Miller, and E. U. Rafailov, "Ultrafast electroabsorption dynamics in an InAs quantum dot saturable absorber at 1.3 μm," Appl. Phys. Lett. **89**(17), 171111 (2006).
6. T. Piwonski, J. Pulka, G. Madden, G. Huyet, J. Houlihan, E. A. Viktorov, T. Erneux, and P. Mandel, "Intradot dynamics of InAs quantum dot based electroabsorbers," Appl. Phys. Lett. **94**(12), 123504 (2009).
7. E. U. Rafailov, M. A. Cataluna, and W. Sibbett, "Mode-locked quantum-dot lasers," Nat. Photonics **1**(7), 395–401 (2007).
8. L. W. Shi, Y. H. Chen, B. Xu, Z. C. Wang, Y. H. Jiao, and Z. G. Wang, "Status and trends of short pulse generation using mode-locked lasers based on advanced quantum-dot active media," J. Phys. D Appl. Phys. **40**(18), R307–R318 (2007).
9. M. G. Thompson, A. R. Rae, M. Xia, R. V. Penty, and I. H. White, "InGaAs quantum-dot mode-locked laser diodes," IEEE J. Sel. Top. Quantum Electron. **15**(3), 661–672 (2009).
10. M. A. Cataluna, Y. Ding, D. I. Nikitichev, K. A. Fedorova, and E. U. Rafailov, "High-power versatile picosecond pulse generation from mode-Locked quantum-dot laser diodes," IEEE J. Sel. of Quantum Electron. **17**(5), 1302–1310 (2011).
11. S. Schneider, U. K. Woggon, P. Borri, W. Langbein, D. Ouyang, R. Sellin, and D. Bimberg, "Ultrafast gain recovery dynamics of the excited state in InGaAs quantum dot amplifiers," in *Conference on Lasers and Electro-Optics/Quantum Electronics and Laser Science and Photonic Applications Systems Technologies*, Technical Digest Series (CD) (Optical Society of America, 2005), paper CThH6.
12. H. C. Schneider, W. W. Chow, and S. W. Koch, "Anomalous carrier-induced dispersion in quantum-dot," Phys. Rev. B **66**(4), 041310 (2002).
13. A. I. O'Driscoll, T. Piwonski, J. Houlihan, G. Huyet, R. J. Manning, and B. Corbett, "Phase dynamics of InAs/GaAs quantum dot semiconductor optical amplifiers," Appl. Phys. Lett. **91**(26), 263506 (2007).
14. P. F. Xu, H. M. Ji, J. L. Xiao, Y. X. Gu, Y. Z. Huang, and T. Yang, "Reduced linewidth enhancement factor due to excited state transition of quantum dot lasers," Opt. Lett. **37**(8), 1298–1300 (2012).

#195145 - $15.00 USD Received 5 Aug 2013; revised 3 Oct 2013; accepted 8 Oct 2013; published 24 Oct 2013

15. M. Kuntz, G. Fiol, M. Laemmlin, C. Meuer, and D. Bimberg, "High-speed mode-locked quantum-dot lasers and optical amplifiers," Proc. IEEE **95**(9), 1767–1778 (2007).
16. M. A. Cataluna, A. R. Kovsh, and E. U. Rafailov, "Stable mode locking via ground- or excited-state transitions in a two-section quantum-dot laser," Appl. Phys. Lett. **89**(8), 081124 (2006).
17. M. A. Cataluna, D. I. Nikitichev, S. Mikroulis, H. Simos, C. Simos, C. Mesaritakis, D. Syvridis, I. Krestnikov, D. Livshits, and E. U. Rafailov, "Dual-wavelength mode-locked quantum-dot laser, via ground and excited state transitions: experimental and theoretical investigation," Opt. Express **18**(12), 12832–12838 (2010).
18. S. Breuer, M. Rossetti, W. Elsässer, L. Drzewietzki, P. Bardella, I. Montrosset, M. Krakowski, and M. Hopkinson, "Reverse-emission-state-transition mode locking of a two-section InAs/InGaAs quantum dot laser," Appl. Phys. Lett. **97**(7), 071118 (2010).
19. T. H. Xu, M. Rossetti, P. Bardella, and I. Montrosset, "Simulation and analysis of dynamic regimes involving ground and excited state transitions in quantum dot passively mode-locked lasers," IEEE J. Quantum Electron. **48**(9), 1193–1202 (2012).
20. S. Breuer, M. Rossetti, L. Drzewietzki, P. Bardella, I. Montrosset, and W. Elsäßer, "Joint experimental and theoretical investigations of two-state mode locking in a strongly chirped reverse-biased monolithic quantum dot laser," IEEE J. Quantum Electron. **47**(10), 1320–1329 (2011).
21. J. Y. Kim, M. T. Choi, W. K. Lee, and P. J. Delfyett, Jr., "Wavelength tunable mode-locked quantum-dot laser," Proc. SPIE **6243**, 1–8 (2006).
22. J. Y. Kim, M. T. Choi, and P. J. Delfyett, "Pulse generation and compression via ground and excited states from a grating coupled passively mode-locked quantum dot two-section diode laser," Appl. Phys. Lett. **89**(26), 261106 (2006).
23. A. E. Zhukov, A. R. Kovsh, V. M. Ustinov, A. Y. Egorov, N. N. Ledentsov, A. F. Tsatsul'nikov, M. V. Maximov, Y. M. Shernyakov, V. I. Kopchatov, A. V. Lunev, P. S. Kop'ev, D. Bimberg, and Z. I. Alferov, "Gain characteristics of quantum dot injection lasers," Semicond. Sci. Technol. **14**(1), 118–123 (1999).
24. X. D. Huang, A. Stintz, H. Li, A. Rice, G. T. Liu, L. F. Lester, J. Cheng, and K. J. Malloy, "Bistable operation of a two-section 1.3-μm InAs quantum dot laser—absorption saturation and the quantum confined stark effect," IEEE J. Quantum Electron. **37**(3), 414–417 (2001).
25. X. D. Huang, A. Stintz, H. Li, L. F. Lester, J. Cheng, and K. J. Malloy, "Passive mode-locking in 1.3 um two-section InAs quantum dot lasers," Appl. Phys. Lett. **78**(19), 2825–2827 (2001).
26. M. G. Thompson, A. Rae, R. L. Sellin, C. Marinelli, R. V. Penty, I. H. White, A. R. Kovsh, S. S. Mikhrin, D. A. Livshits, and I. L. Krestnikov, "Subpicosecond high-power mode locking using flared waveguide monolithic quantum-dot lasers," Appl. Phys. Lett. **88**(13), 133119 (2006).
27. M. A. Cataluna, E. U. Rafailov, A. D. McRobbie, W. Sibbett, D. A. Livshits, and A. R. Kovsh, "Stable Mode-Locked Operation up to 80 °C From an InGaAs Quantum-Dot Laser," IEEE Photon. Technol. Lett. **18**(14), 1500–1502 (2006).
28. L. W. Jiang, X. L. Ye, X. L. Zhou, P. Jin, X. Q. Lü, and Z. G. Wang, "Optical bistability in a two-section InAs quantum-dot laser," J. Semicond. **31**(11), 114012 (2010).
29. H. Kawaguchi, "Absorptive and dispersive bistability in semiconductor injection lasers," Opt. Quantum Electron. **19**(S1), S1–S36 (1987).
30. M. Ueno and R. Lang, "Conditions for self-sustained pulsation and bistability in semiconductor lasers," J. Appl. Phys. **58**(4), 1689–1692 (1985).
31. S. Arahira and Y. Ogawa, "Repetition – frequency tuning of monolithic passively mode-locked semiconductor lasers with integrated extended cavities," IEEE J. Quantum Electron. **33**(2), 255–264 (1997).
32. F. Kéfélian, S. O'Donoghue, M. T. Todaro, J. McInerney, and G. Huyet, "Experimental investigation of different regimes of mode-locking in a high repetition rate passively mode-locked semiconductor quantum-dot laser," Opt. Express **17**(8), 6258–6267 (2009).
33. G. Carpintero, M. G. Thompson, K. Yvind, R. V. Penty, and I. H. White, "Comparison of the noise performance of 10 GHz repetition rate quantum-dot and quantum well monolithic mode-locked semiconductor lasers," IET Optoelectron. **5**(5), 195–201 (2011).
34. T. Piwonski, J. Pulka, E. A. Viktorov, G. Huyet, and J. Houlihan, "Refractive index dynamics of quantum dot based waveguide electroabsorbers," Appl. Phys. Lett. **97**(5), 051107 (2010).
35. K. A. Williams, M. G. Thompson, and I. H. White, "Long-wavelength monolithic mode-locked diode lasers," New J. Phys. **6**, 179 (2004).
36. E. B. Treacy, "Optical pulse compression with diffraction gratings," IEEE J. Quantum Electron. **5**(9), 454–458 (1969).

1. Introduction

Using quantum dots (QD) as active media for semiconductor lasers has been extensively studied for over a decade. Because of quantized energy states, limited density of states (or density of QD), and finite intraband relaxation time, gain clamping does not exist in QD lasers [1]. Thus, QD lasers are capable of ground-state, excited-state, or simultaneously two-state lasing depending on the operation condition, cavity structure, characteristics of QDs, and other structural parameters [2,3]. Several studies have shown [4–6], both the ground and the

#195145 - $15.00 USD Received 5 Aug 2013; revised 3 Oct 2013; accepted 8 Oct 2013; published 24 Oct 2013

excited-state transitions have subpicosecond gain and absorption recovery time. With the fast carrier dynamics and inherent broadband gain, QDs have been extensively used for mode-locked lasers to generate ultra-short pulses [7–10]. While most of the works were focused on the ground-state transition, some experimental results have indicated that using the excited-state transition for mode-locking operation may have the potential for achieving shorter and chirpless pulses. A faster absorption recovery time [6], and a small or a negative linewidth enhancement factor have been reported for the excited-state transitions [11–14]. The higher saturated gain and faster absorption recovery rate could also be beneficial to achieve higher repetition rates in mode-locked lasers [15]. Cataluna et al. demonstrated passive mode-locking via ground- or excited-state transition in a monolithic QD laser [16,17]. However, the excited-state mode-locking was achieved at the expense of a high injection current, which significantly broadened the pulses. The minimum pulsewidth for the excited-state transition was 7 ps with a spectral width of 5.5 nm. Breuer et al. demonstrated a 3.3 ps pulsewidth using a chirped-QD active media [18–20]. Kim et al. used an external-cavity arrangement to select the excited-state transition and obtained a minimum pulsewidth of ~11 ps, which was then compressed to 1.2 ps [21,22].

In this paper, we report results on a comprehensive study of a passive mode-locked QD laser based on the excited-state transition in a monolithic two-section structure. By choosing a suitable cavity length, we were able to obtain only the excited-state lasing and mode-locking with a significantly reduced threshold current. Characteristics of these mode-locked lasers were studied in detail at different levels of injection current and absorber bias. Decreasing of hysteresis width with absorber bias, optical spectra narrowing and anomalous evolution of repetition frequency were observed in our lasers and different from conventional mode-locked QD lasers via ground-state transition. A minimum pulsewidth of 3.3 ps and an externally compressed pulsewidth of 0.78 ps were obtained.

2. Device structure and experiments

The lasers investigated in this work were grown on (001) n^+-GaAs substrates with a Veeco Gen II molecular beam epitaxy system. The active region consisted of seven 2.6-monolayer InAs-QD layers, and each of them was capped with a 5 nm-thick $In_{0.15}Ga_{0.85}As$ strain-reducing layer and separated by a 45 nm-thick GaAs spacer. The active region was placed in the center of a GaAs matrix as an optical-waveguide core in a total thickness of 540 nm and was sandwiched between two 1.4 μm-thick $Al_{0.4}Ga_{0.6}As$ cladding layers. The dot density was around $1*10^{10}/cm^2$.

The devices were fabricated into 4.5 μm-wide ridge waveguides using a dry-etching process. Single-section and two-section Fabry-Pérot lasers with cavity lengths of 1 mm up to 3 mm were fabricated. For the two-section lasers, the absorber-to-gain length ratio varied from 1:5 to 1:9. A trench of 5 μm-wide and 600 nm-deep (~200 nm into the p-cladding layer) was etched between the two sections. The trench ensured an electrical isolation while kept the optical scattering loss to a minimum. The resistance measured between the two sections was 3 kΩ. The two side mirrors of the resonant cavity were formed by cleavage without any coating.

Figure 1(a) shows the room temperature photoluminescence (PL) spectra measured at different pumping powers and lasing spectra for the ground and the first excited-state lasers. In the PL spectra, several peaks corresponding to the ground and several excited states were clearly observable. The lasing spectra were obtained from two separate single-section lasers, one with a cavity length of 2 mm for the ground-state lasing at a wavelength of 1295 nm, and the other with a cavity length of 1.5 mm for the excited-state lasing at 1218 nm. Both lasers were operated at an injection current, which was two times of the threshold current. The threshold current was 17.5 mA and 30 mA for the ground state and the excited state, respectively. With further increasing the current larger than two times the threshold current in

#195145 - $15.00 USD Received 5 Aug 2013; revised 3 Oct 2013; accepted 8 Oct 2013; published 24 Oct 2013

the 2-mm-long laser, the excited-state lasing would also occur and then quench the ground-state lasing.

Single-section lasers with different cavity lengths were used to extract the saturated gain (G_0) and the transparency current density (J_0) [23]. Figure 1(b) shows the modal gain and the lasing wavelength as functions of the threshold current density. Both the experimental data and the fitted curves are shown, and the peak wavelength was measured at threshold. The extracted saturated gains were 12.6 cm^{-1} and 22.3 cm^{-1} for the ground state and the excited state respectively, and the corresponding transparency current densities were 30 A/cm^2 and 130 A/cm^2. The additional fitting parameter, gamma, is dimensionless and can be treated as a non-ideality parameter.

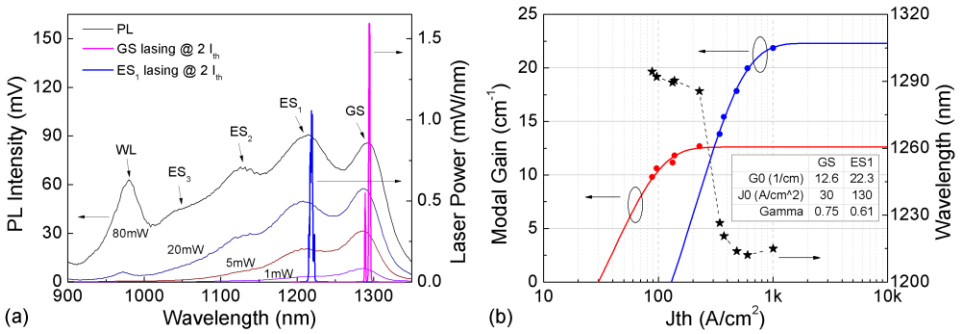

Fig. 1. (a) PL spectra of the QD sample and lasing spectra of single-section lasers. (b) Modal gain and lasing wavelength as functions of current density. (dots: experimental data; lines: fitting curves).

Passive mode-locking was achieved with the two-section cavity design. Since we focused on mode-locking via the excited-state transition, cavities were chosen so that only the excited-state lasing was present. Because the threshold modal gain of the 2-mm-long single-section laser was very close to the ground-state saturated gain, the excited-state lasing can be easily achieved by biasing the absorber section with voltages lower than that of the gain section. We have confirmed experimentally there was no ground-state lasing for all 2-mm-long two section devices with length ratios from 1:5 to 1:9 when the absorber bias was at + 1 V or lower. In this paper, we focus on the devices with a 2-mm-long cavity and a length ratio of 1:5. The static characteristic of the output power versus the injection current (L-I curve) with different absorber bias voltages was measured with a multi-channel semiconductor device analyzer (Agilent B1500A). Optical spectra and RF spectra of photo-current were measured simultaneously. The laser output was coupled into an inline fiber isolator, which was followed by a fiber coupler that diverts 10% of the power to an optical spectrum analyzer (Ando AQ6315E, minimum resolution of 0.05 nm). The rest 90% went into a 35 GHz-bandwidth photo-receiver (Newport AD-10ir), which was followed by a 26.5-GHz electrical spectrum analyzer (Agilent E4407B). The pulsewidth was measured by a background-free intensity autocorrelator (Femtochrome FR-103XL).

3. Results and discussion

3.1 Static L-I curves and hysteresis

Figure 2 shows the L-I curves with the absorber bias varied from + 1 V to −8 V. Through the operation region, only excited-state lasing was observed, which was confirmed with the optical spectra. The thick line in the figure is the forward trace with current swept from low to high, and the thin line is the backward trace with current swept from high to low. Hysteresis and unstable regions were observed near the threshold. The hysteresis is due to the presence of saturable absorption, where the loss in the absorber is reduced when the laser turns on or

#195145 - $15.00 USD Received 5 Aug 2013; revised 3 Oct 2013; accepted 8 Oct 2013; published 24 Oct 2013

when an intense light passes through. Unlike the commonly observed hysteresis of mode-locked lasers via ground-state transition, where the width of the hysteresis loop increases when the absorber reverse bias is increased [24–27], the hysteresis width of the excited-state mode-locked lasers decreases with the absorber bias. A similar result was observed in a two-section QD laser with continuous-wave lasing via ground-state transition [28]. Here, we demonstrate a clear evolution of the hysteresis relative to the absorber bias in excited-state mode-locked lasers. It is also noteworthy that the output power near the threshold of the backward trace is nearly constant with the absorber bias voltage varied from + 1 V to −3V. It corresponds to a minimum pulse energy of 0.12 pJ required to saturate the absorber. We believe that the constant pulse energy in our device is due to an ultrafast recovery of the excited-state absorption even under a low reverse bias, and the absorption recovery is efficient in the monolithic laser for a medium cavity roundtrip time around 50 ps.

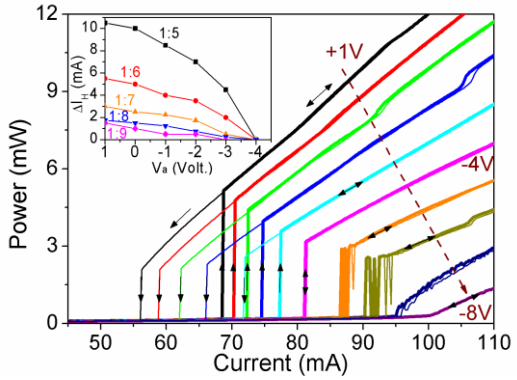

Fig. 2. L-I curves with the absorber bias swept from + 1 V to −8 V. Inset: hysteresis widths of mode-locked lasers with different length ratios as a function of the absorber bias.

Hysteresis widths of devices with different absorber-to-gain length ratios (but with the same cavity length of 2 mm) are shown in the inset of Fig. 2. In all cases the width decreases with the reverse bias. The width of the hysteresis and its rate of change go down as the ratio decreases. Despite the different length ratio, the hysteresis disappears at about the same reverse bias of −4 V. For devices with a cavity length longer than 2 mm, the vanishing point of the hysteresis goes beyond −4 V. We have confirmed, with the measurements of RF spectra and the pulse width, the mode-locked state was maintained during the bistability. When the absorber reverse bias goes beyond −4 V, strong oscillations in the L-I curves are observed near the threshold. In this situation, the mode-locking was accompanied by a low-frequency self-pulsation. When the pumping current was increased, the frequency of oscillation increased gradually from several tens of Hz to a few kilo-Hz. Because of the slow oscillation, this unstable region can be clearly defined using measurements with different integration times. With further increase of the reverse bias, Q-switching modulated mode-locking occurs and small fluctuations can be seen on the L-I curves. However, the frequency of the Q-switching modulated mode-locking is high (hundreds of MHz), the region cannot be directly defined by the static-LI measurement. We have checked the RF spectra of the photocurrent in the unstable regions to identify the modulation schemes and to measure frequencies.

The intensity bistability and Q-switching behaviors have been studied for two-section lasers before [29]. To explain the relationship between the hysteresis and the absorber bias in our excited-state mode-locked lasers, a simple rate-equation model proposed by Ueno and Lang [30] can be used. In their static analysis, the bistability occurs when the following condition is satisfied:

#195145 - $15.00 USD Received 5 Aug 2013; revised 3 Oct 2013; accepted 8 Oct 2013; published 24 Oct 2013

$$\frac{\tau_g}{\tau_{a,eff}}\frac{\partial g/\partial n}{\partial \alpha/\partial n} < \frac{\beta}{1+\beta}. \quad (1)$$

where τ_g and $\partial g/\partial n$ are the carrier lifetime and the differential gain in the gain section respectively, while $\tau_{a,eff}$ and $\partial \alpha/\partial n$ are the effective carrier lifetime and the differential loss in the absorber section. β is the relative unsaturated absorption defined by the ratio of the unsaturated loss in the absorber to the total cavity loss and is larger for excited state than for ground state under the same absorber bias. However, it actually plays a minor role. In the model, hysteresis width becomes wider when the left-hand side value of the equation decreases. $\partial \alpha/\partial n$ could increase in ground state but decrease in excited state when the reverse bias increases [19], but the changes are relatively small comparing with $\partial g/\partial n$. The most important factors are $\tau_{a,eff}$ and $\partial g/\partial n$, which both decrease when the reverse bias increases. The former is due to the increased thermionic emission or tunneling rates [6], and the latter is due to the gain-saturation effect (see Fig. 1(b)).

For ground state mode-locked lasers, a larger hysteresis is usually observed under a high reverse bias due to the strong gain-saturation effect, where the differential gain decreases rapidly. However, if the absorber recovery time goes down faster than the differential gain as the reverse bias of the absorber increases, it significantly increases the non-saturable loss and the threshold current of the backward traces. The hysteresis region then tends to decrease and eventually disappear. This is exactly the case observed here in our mode-locked lasers, where the excited-state transition has a higher differential gain and a shorter absorber recovery time than the ground-state transition.

3.2 Characteristics of optical and electrical spectra

We have mapped the mode-locked region of our device in two dimensional plots, with Fig. 3(a) in the wavelength-current plane and Fig. 3(b) in the frequency-current plane. The color scale shows the intensity (in log scale) of the mode-locked pulses. The injection current for the gain region was varied from the threshold of 82 mA to 210 mA. The absorber bias was fixed at −5 V. It is seen from Fig. 3(a) that the laser's center wavelength increases with the injection current throughout the measured range. It is noticed that a wavelength jump occurred at 95 mA with a wavelength difference of 4 nm. This is probably due to the existence of two clusters of longitudinal modes [32] in the excited state transition. When the current is near the threshold but below 95 mA, the cluster of short-wavelength modes, named M1, dominate, but the mode-locking is not stable and it is accompanied by a low-frequency self-pulsation and there is a competition between the two clusters of longitudinal modes. When the current is above 95 mA, stable mode-locking is obtained and the wavelength shifts to that of the cluster of long-wavelength modes (named M2). The vertical dash lines mark the boundary between the unstable mode-locked region and the stable mode-locked region. The instability at low currents is the same as that shown in the L-I curves in Fig. 2 when the absorber is at high reverse biases. Looking carefully at Fig. 3(a), we noticed there was some modulation in the spectra affecting the linewidth at a high injection current. The full width at half maximum (FWHM) of the optical spectrum is shown in Fig. 3(a) by the white dots with the scale shown on the right axis. The FWHM first increases to a maximum value of 5.1 nm at 130 mA and then decreases to 1.3 nm at 210 mA. The increase of injection current or power usually leads to a spectral broadening due to the self-phase modulation effect. Instead of that, the anomalous spectral narrowing occurred when the output power still went up. However, the reason is still not clear at this moment.

The RF spectra in Fig. 3(b) were measured with a 500-MHz span and a resolution bandwidth of 300 kHz. Only one peak without Q-switching modulation is clearly observed in this range. In the M1 region to the left of 95 mA, the repetition frequency increases with the

#195145 - $15.00 USD Received 5 Aug 2013; revised 3 Oct 2013; accepted 8 Oct 2013; published 24 Oct 2013

injection current. (It should be noted that the low-frequency self-pulsation observed in Fig. 2 accompanies the mode-locking in this region. However, the electrical spectrum analyzer does not detect the low modulation frequency.) A frequency jump of 17.6 MHz is observed and corresponding to the wavelength jump at the boundary. This frequency increase can be attributed to the lowering of the effective refractive index as the wavelength shifts longer. The 4 nm wavelength difference and the accompanying 17.6 MHz frequency change correspond to a linear waveguide dispersion of $-8.3*10^{-4}$ / nm. In the M2 region, the repetition frequency decreases with an average rate of −37 kHz*cm^2/A. The tuning range of the repetition rate is around 47 MHz, which is 0.29% of the repetition frequency. The evolution of the Lorentz-fitted RF linewidth is also shown in Fig. 3(b) in a log scale. The measurement was done with an 80-MHz span and a 30-kHz resolution bandwidth. The RF linewidth was observed to decrease with the increase of the injection current. It can be attributed to the decrease of the relative noise when the power increases. The narrowest linewidth is 6.63 kHz with an integrated RMS timing jitter of 364 fs (1 MHz to 40 MHz), which is slightly larger than that typically obtained in ground-state mode-locked lasers [33]. This is due to a higher carrier population for excited-state lasers, which leads to a higher level of spontaneous emission.

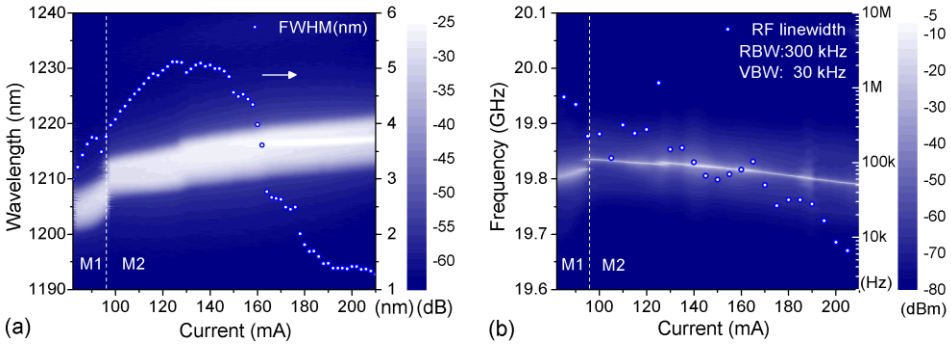

Fig. 3. (a) Optical spectra relative to the injection current (dots: FWHM of the optical spectra), (b) RF spectra relative to the current (dots: Lorentz-fitted −3dB RF linewidth). The absorber bias is fixed at −5 V. The color scale shows the intensity in a log scale.

3.3 Evolution of electrical spectra

Different tuning rates of the repetition frequency have been reported for mode-locked QD lasers via ground-state transition [15,25,32]. The frequency tuning could be attributed to the waveguide dispersion, the carrier density induced refractive index change, and the pulse energy caused frequency detuning [31]. In passively mode-locked semiconductor lasers, the relationship between RF/optical spectra and the bias condition is complicated. Kéfélian et al. reported an increase of repetition frequency together with a wavelength red-shift as the current increases. For our devices, wavelength red shift and repetition frequency increase happened together only in the small region of M1. In the dominant and stable mode-locked region of M2, an anomalous relation between the repetition frequency and the lasing wavelength is observed. In this region, the repetition frequency decreases but the wavelength red shifts when the injection current increases. Similar results were observed in our device with different absorber biases. This phenomenon cannot be explained by the various dispersion effects mentioned above. If we considered the thermal expansion in gallium arsenide, the frequency of a 20-GHz repetition-rate laser could change by a rate of ~-114 kHz/°C owning to the change of the cavity length. When the injection current in Fig. 3(b) changed from 100 mA to 200 mA, the repetition frequency changed by −40 MHz, which is too large to be caused only by the temperature effect. Here, we propose that the decrease of the repetition frequency could be due to a positive differential refractive index which has been observed at the excited-state of QD amplifiers [11,12] and waveguide electro-absorbers [34].

#195145 - $15.00 USD Received 5 Aug 2013; revised 3 Oct 2013; accepted 8 Oct 2013; published 24 Oct 2013

In a static condition, the carrier density is not clamped in QD lasers when the injection current increases [1]. An increase of refractive index would occur when a positive differential refractive index exists in the gain section. The increase of refractive index then could lead to an increase of group index and decrease of group velocity. Thus, the increase of gain current could accompany a decrease of the repetition rate. The positive differential refractive index is also beneficial for optical mode restriction and can lead to a negative linewidth enhancement factor.

3.4 Autocorrelation traces and two-dimensional mapping of pulsewidth

The pulsewidth of the mode-locked pulses was measured using the background-free intensity autocorrelation technique. Figure 4(a) shows the autocorrelation traces of the mode-locked pulses in a logarithmic scale. The device was operated with an absorber bias of –5 V, and the gain current was varied from 85 mA to 200 mA. The pulses can be fitted very well with a squared hyperbolic secant ($sech^2$) function. The red dash lines are the fitted curves. Pulse trains with a longer time domain at gain currents of 100 mA and 150 mA are shown in the inset, and the nearly 50-ps period corresponds correctly to the cavity's roundtrip time.

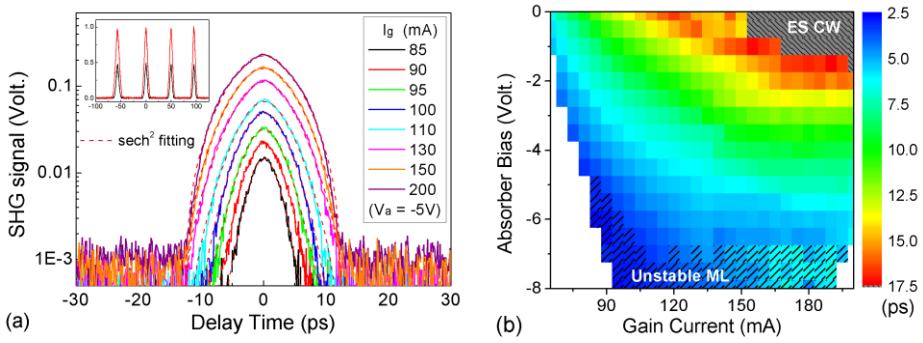

Fig. 4. (a) Autocorrelation traces in a log scale at different gain currents while the absorber bias is –5 V. Inset: long traces in a linear scale (b) 2D-Mapping of pulsewidths as functions of gain current and absorber bias.

Figure 4(b) shows a two-dimensional mapping of the de-correlated pulsewidth as a function of the gain current and the absorber bias. The white region represents the non-lasing state. The unstable mode-locked region, in which mode-locking is usually accompanied by a self-pulsation or a Q-switching modulation, is painted with left-oblique lines. When the pulsewidth is larger than 17.5 ps, we define it as CW-lasing or incomplete mode locking, which is represented by the dark-gray region. The pulsewidth decreases when the reverse bias of the absorber is increased and the gain current is reduced. Pulse shortening is due to a shorter absorption recovery time at higher reverse bias, which results in a reduction of the time window where the pulse experiences a net gain [35]. On the contrary, when the gain current increases, the net-gain window becomes larger because of a faster gain recovery time. The minimum pulsewidth of 2.8 ps occurred near the threshold when the reverse bias was larger than –6 V. However, mode-locking at the condition was accompanied by a low frequency self-pulsation or Q-switching modulation. In the stable mode-locked region, the minimum pulsewidth was 3.3 ps with a peak power of 45 mW, and it was operated with an injection current of 95 mA and an absorber bias of –6 V. The corresponding time-bandwidth product was 1.52, which was about 5 times of the Fourier-transform limited value and suggested the pulse was still highly chirped.

#195145 - $15.00 USD Received 5 Aug 2013; revised 3 Oct 2013; accepted 8 Oct 2013; published 24 Oct 2013

3.5 Time-bandwidth product, peak power, and pulse compression

Figure 5(a) shows the time-bandwidth product and the peak power with the absorber bias fixed at –5 V. The time-bandwidth product increases from 2.0 near the threshold to 6.18 at 140 mA and then decreases to a minimum value of 1.85 at 195 mA, while the peak power and the average power increase throughout the measured current range. The significant reduction of the time-bandwidth product at high currents is due to the reduction of spectral linewidth as shown in Fig. 3(a). The maximum peak power is 103 mW with a corresponding pulsewidth of 6.5 ps and a time-bandwidth product of 1.88. For ground-state mode-locked lasers [7,8], the peak power is typically in the range from mW to W. Compared with them, the peak power achieved for our ES mode-locked lasers is comparable to those of conventional mode-locked QD lasers.

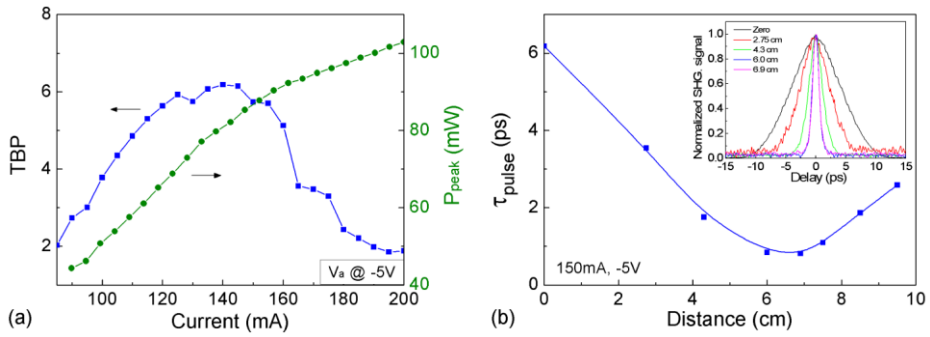

Fig. 5. (a) Time-bandwidth product and peak power as functions of gain current with the absorber bias fixed at –5 V. (b) Pulsewidth as a function of the distance between the two gratings. Inset: normalized autocorrelation traces with the distance from 0 to 6.9 cm.

To understand the chirp in the mode-locked pulses and to determine its sign, the pulses were compressed by a double-grating pulse compressor [36] and then measured by an autocorrelator. Only negative and near-linear chirp can be introduced by the setup. The introduced linear chirp is proportional to the distance between the two gratings. We use the distance to represent the relative chirp. Figure 5(b) shows the pulsewidth relative to the distance, while the injection current and the absorber bias were 150 mA and –5 V, respectively. Pulse compression was obtained until the distance reaches 6.9 cm, and then the pulses broadened with further increase of the distance. The corresponding autocorrelation traces are shown in the inset. Since our setup only introduces negative chirp, the output pulses are positively chirped (up-chirp). The minimum compressed pulsewidth is 0.78 ps, and the corresponding time-bandwidth product is 0.8, which has been the shortest pulse achieved in mode-locked QD lasers via excited-state transition.

4. Conclusion

In summary, we have demonstrated a QD mode-locked laser via only the excited-state transition in a broad operating range. Without competing with the ground-state transition, the threshold current is significantly lowered, and the mode-locked region is stable. A minimum pulsewidth of 3.3 ps was obtained. We observed a decrease of hysteresis width in the L-I curve when the reverse bias of the absorber was increased. This is due to a faster absorber recovery rate and a higher saturated gain for the excited state relative to those of the ground state. An anomalous relation between the repetition frequency and the lasing wavelength, a spectral narrowing and a decrease of time-bandwidth product were also observed when increasing the gain current. It could be due to a positive differential refractive index for the excited-state transition and could lead to a negative linewidth enhancement factor. With an external compression, we obtained a minimum pulsewidth of 0.78 ps, and the uncompressed

#195145 - $15.00 USD Received 5 Aug 2013; revised 3 Oct 2013; accepted 8 Oct 2013; published 24 Oct 2013

pulse was still up-chirped. The investigation of mode-locking via the excited-state transition helps us to understand and potentially fully use the spectral versatility of QDs.

Acknowledgments

This research was supported by the National Science Council of Taiwan under Grant No. NSC 101-3113-P-009-004. The authors would like to thank the help from Center for Nano Science and Technology (CNST) of National Chiao Tung University.

#195145 - $15.00 USD Received 5 Aug 2013; revised 3 Oct 2013; accepted 8 Oct 2013; published 24 Oct 2013